REFRACTORY INCLUSION SIZE DISTRIBUTION AND FABRIC MEASURED IN A LARGE SLAB OF THE ALLENDE CV3 CHONDRITE.

P. Srinivasan[1], J. I. Simon[2], J. N. Cuzzi[3], [1]University of New Mexico, Department of Earth and Planetary Sciences, Albuquerque, NM, 87131, psrinivasan@unm.edu, [2]Center for Isotope Cosmochemistry and Geochronology, ARES, NASA JSC, Houston, TX 77058, justin.i.simon@nasa.gov, [3]NASA Ames, Moffett Field, CA 94035, jeffrey.cuzzi@nasa.gov.

Introduction: Aggregate textures of chondrites reflect accretion of early-formed particles in the solar nebula. Explanations for the size and density variations of particle populations found among chondrites are debated. Differences could have risen out of formation in different locations in the nebula, and/or they could have been caused by a sorting process [1]. Many ideas on the cause of chondrule sorting have been proposed; some including sorting by mass [2,3], by X-winds [4], turbulent concentration [5], and by photophoresis [6]. However, few similar studies have been conducted for Ca-, Al-rich inclusions (CAIs). These particles are known to have formed early, and their distribution could attest to the early stages of Solar System (ESS) history. Unfortunately, CAIs are not as common in chondrites as chondrules are, reducing the usefulness of studies restricted to a few thin sections. Furthermore, the largest sizes of CAIs are generally much larger than chondrules, and therefore rarely present in most studied chondrite thin sections. This study attempts to perform a more representative sampling of the CAI population in the Allende chondrite by investigating a two decimeter-sized slab.

Allende CV3 chondrite. Allende is classified as a carbonaceous chondrite, under the Vigarano specimen type. Allende was heated to about 550 - 600°C [7], probably resulting from shock [8] or short-lived isotopes [9]. Due to its exposure to heat, some argue that this sample is not pristine enough to study primary processes in the solar nebula, as it has encountered secondary processes. Whilst that may be true in some context, understanding the initial stages of an object is unattainable without understanding its consequential stages. Furthermore, this is less of a concern for textural analysis studies that rely on the shape, size, and distribution of particles rather than for compositional or mineralogical analyses.

Methodology: For our analyses, we used a large slab of the Allende CV3 chondrite (~26 cm x 20 cm).

Macro-photographs. In order to accurately constrain the distribution of the largest CAIs in Allende, measurement of a large slab is required. In practical terms, analyses of more than 10 thin sections would be required to represent the anticipated size distribution of CAIs [10]. A large Allende slab has been located in a private collection and made available for non-destructive investigation. Our analyses mainly derive from examining particles with high-resolution digital macro-photographs (5.4μm/pixel), using a camera

attached to a petrologic microscope. Both the front and back of the slab have been photographed with 1.25x magnification. Due to the roughness of the cut of the slab, this was determined to be the best magnification to focus on the individual particles. Roughly 400 images for each side were produced and stitched together (Figure 1). All of the CAIs on both sides of the slab seen have been outlined digitally. Previously studied macro-photographs on Allende helped with the identification of the CAIs.

Figure 1. *A side of the studied Allende slab under plain light. Each side reflects a mosaic of ~400 photos.*

Since no mineralogical data has yet been taken for the slab, there will in essence be an error in the count, since some CAIs might have been spuriously excluded and some other particles might have been included. Our preliminary analysis at NASA Johnson Space Center shows that CAIs and chondrules (and chondritic matrix) could be distinguished with X-ray computed Tomography (CT scanning) [e.g., 11,12]. A comparable density-based size frequency and particle distribution data set will be obtained shortly. Likewise, integration of the micro-scale X-ray mapping performed by [13] with the macrophotography analysis will be pursued. This will provide particle sizes to be evaluated as small as ~50 μm. Ultimately these data will be processed by matrix inversion to transform 2-D particle section areas into volumes (i.e., unfolded, [13]) to get a more accurate particle size distribution. Any such integration will require proper scaling, which is still being worked out.

ImageJ. Outlining all of the CAIs and chondrules allows us to create a binary image of the samples (Figure 2). We can then use the image analysis program ImageJ to characterize the particles, in particular their sizes. Based on the binary data, ImageJ

produces data for the area of each particle, its location in the slab, as well as its major and minor axes. In the current study, we excluded particles that were under 200000 μm^2 in size. Identification of smaller particles are less certain by eye and the smaller sizes will be obtained from integrating a coordinated X-ray mapping study performed last year [13].

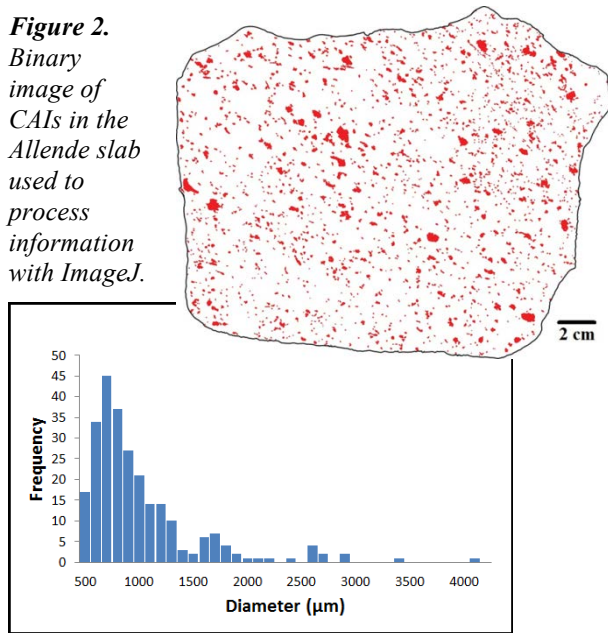*Figure 2. Binary image of CAIs in the Allende slab used to process information with ImageJ.*

2 cm

Figure 3. Particle count distribution for CAIs in the Allende slab according to diameter (in μm). Smallest particle size accounted for was ≥200,000 μm².

Results: *Size frequency histogram.* With ImageJ, we produce data for the mean particle size as well as a histogram of the CAIs (Figure 3). Below lists the overall statistics:

- Number of particles traced (n) = 513
- Mean area = 571262.96 μm^2 (0.6% total)
- Standard deviation = 708571.4 μm^2
- Min axis = 496.2 μm
- Max axis = 4119.0 μm
- Preferred orientation ~145°

Rose diagram. After obtaining the ImageJ particle count distributions, we created a rose diagram to document the frequency of lineations in a given orientation for CAIs in the Allende slab. Figure 4 below shows a strong fabric in the slab, with a preferred orientation of CAIs trending ~145°.

Discussion and Future Work: At face value, similar to chondrule size populations reported for Allende [14,15], there is a much higher frequency of smaller sized CAIs than larger ones, which could mean that CAIs and chondrules were sorted by the same or similar processes. Current estimates show CAI as 0.6%

of total area of the slab, while our estimates of smaller CV samples showed an estimate of 2.6% [13]. Chondrule area fractions, which are not included yet in this study, are increasingly larger in these samples, with estimates of ~57%. Our CAI modal size is also comparable to the modal peak of chondrules from the literature [16,17].

Circle = 7 %

Figure 4. Half rose diagram (180°) of the Allende slab. The angle of the major axes are defined between 0°-180°, and match the slab orientation in Figs. 1 & 2.
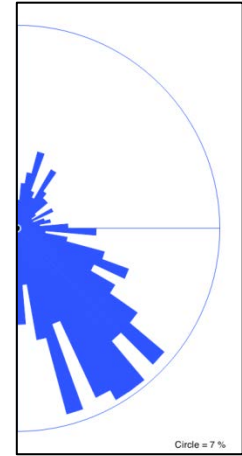
Previous research of ordinary chondrites and some achondrites has shown that that there is a correlation between the degree of collective orientation of particles to shock loading [18], which might in fact explain our new data as well. Due to the large size of the Allende slab, all data obtained from these CAIs have the advantage over existing estimates and their related interpretations for CAI sorting processes in the ESS. Having macro-photographs of the Allende slab is necessary in measuring the proportion of largest CAIs in the Allende population, however, more data must be obtained as well. CT scanning will also immensely add to this project, as it will give us more quantitative analyses providing more robust identification of smaller particles.

References: [1] Jones R. H. (2005) *ASP, 341,* 251-281. [2] Teitler S. A. et al. (2010) *MPS, 45,* 1124-1135. [3] Cuzzi J. N. et al. (2001) *APJ, 546,* 496-508. [4] Shu F. H. et al. (1996) *Science, 271,* 1545-1552. [5] Hogen R. C. et al. (1999) *Physical Rev. E, 60,* 1674-1680. [6] Wurm G. & Krauss O. (2006), *Icarus, 180,* 487-495. [7] Bonal L. et al. (2006) *GCA, 70,* 1849-1863. [8] Rubin A. E. (2005) *Sci. Am., 292,* 80-87. [9] Scott E. R. D. (2007) *Annu. Rev. Earth Planet. Sci., 35,* 577-620. [10] Chayes F. (1956) in *Petrologic Modal Analysis,* 1-139. [11] Ebel D. S. et al. (2009) *LPSC, 40,* #2065. [12] Ebel D. S. et al. (2008), *LPS, 39,* #2121. [13] Christoffersen P. A. et al. (2011) *LPS, 43,* #2058. [14] Rubin A. E. (2000) *E.Sci. Rev., 50,* 3-27. [15] Connolly H. C. Jr. & Desch S. J. (2004) *Chem. Erde, 64,* 95-125. [16] Teitler S. A. et al. (2009) *MAPS.* [17] Paque J. M. & Cuzzi J. N. (1997), *LPS, 28,* #1189. [18] Friedrich J. M. et al (2008) *EPSL, 275,* 172-180.